

# Supplementary data

## Rhenium(I) Terpyridine Complexes – Synthesis, Photophysical Properties and Application in Organic Light Emitting Devices.

Tomasz Klemens<sup>a</sup>, Anna Świtlicka-Olszewska<sup>a</sup>, Barbara Machura<sup>a\*</sup>, Marzena Grucela<sup>b</sup>, Ewa Schab-Balcerzak<sup>b\*</sup>, Karolina Smolarek<sup>c</sup>, Sebastian Mackowski<sup>c</sup>, Agata Szlapa<sup>d</sup>, Sławomir Kula<sup>d</sup>, Stanisław Krompiec<sup>d</sup>, Piotr Łodowski<sup>e</sup>, Karol Erfurt<sup>f</sup> and Anna Chrobok<sup>f</sup>

<sup>a</sup>Department of Crystallography, Institute of Chemistry, University of Silesia, 9<sup>th</sup> Szkolna St., 40-006 Katowice, Poland, E-mail: bmachura@poczta.onet.pl

<sup>b</sup>Centre of Polymer and Carbon Materials, Polish Academy of Sciences,  
34 M. Curie-Skłodowska Str., 41-819 Zabrze, Poland

<sup>c</sup>Institute of Physics, Faculty of Physics, Astronomy and Informatics, Nicolaus Copernicus University, 5 Grudziadzka Str., 87-100 Toruń,  
Poland

<sup>d</sup>Department of Inorganic, Organometallic Chemistry and Catalysis, Institute of Chemistry, University of Silesia, 9<sup>th</sup> Szkolna St., 40-006  
Katowice, Poland

<sup>e</sup>Department of Theoretical Chemistry, Institute of Chemistry, University of Silesia, 9<sup>th</sup> Szkolna St., 40-006 Katowice, Poland

<sup>f</sup>Department of Chemical Organic Technology and Petrochemistry, Silesian University of Technology, Krzywoustego 4, 44-100 Gliwice,  
Poland

**Tables:**

**Table S1.** Crystal data and structure refinement of **2**, **3** and **4** complexes.

**Table S2.** The experimental bond lengths [Å] and angles [°] for the rhenium(I) complexes.

**Table S3.** Short intra- and intermolecular contacts detected in the structures of the tricarbonyl rhenium(I) complexes.

**Table S4.** Comparison of experimental and theoretical bond lengths [Å] and angles [°] for **2**, **3** and **4**.

**Table S5.** Frontier molecular orbital composition (%) in the ground state for complex **1** calculated at the DFT/B3LYP/DEF2-TZVPD level.

**Table S6.** Frontier molecular orbital composition (%) in the ground state for complex **2** calculated at the DFT/B3LYP/DEF2-TZVPD level.

**Table S7.** Frontier molecular orbital composition (%) in the ground state for complex **3** calculated at the DFT/B3LYP/DEF2-TZVPD level.

**Table S8.** Frontier molecular orbital composition (%) in the ground state for complex **4** calculated at the DFT/B3LYP/DEF2-TZVPD level.

**Table S9.** Frontier molecular orbital composition (%) in the ground state for complex **5** calculated at the DFT/B3LYP/DEF2-TZVPD level.

**Table S10.** Frontier molecular orbital composition (%) in the ground state for complex **6** calculated at the DFT/B3LYP/DEF2-TZVPD level.

**Table S11.** The energies and characters of the selected spin-allowed electronic transitions for **1** calculated with the TDDFT/B3LYP method, together with assignment to the experimental absorption bands.

**Table S12.** The energies and characters of the selected spin-allowed electronic transitions for **2** calculated with the TDDFT/B3LYP method, together with assignment to the experimental absorption bands.

**Table S13.** The energies and characters of the selected spin-allowed electronic transitions for **3** calculated with the TDDFT/B3LYP method, together with assignment to the experimental absorption bands.

**Table S14.** The energies and characters of the selected spin-allowed electronic transitions for **4** calculated with the TDDFT/B3LYP method, together with assignment to the experimental absorption bands.

**Table S15.** The energies and characters of the selected spin-allowed electronic transitions for **5** calculated with the TDDFT/B3LYP method, together with assignment to the experimental absorption bands.

**Table S16.** The energies and characters of the selected spin-allowed electronic transitions for **6** calculated with the TDDFT/B3LYP method, together with assignment to the experimental absorption bands.

**Table S17.** Calculated phosphorescence emission energies of **1-6**, compared to the experimental values (in MeCN).

**Figures:**

**Figure S1.** A view of the crystal packing showing intermolecular π–π stacking interactions for **2** and **3**.

**Figure S2.** 1D supramolecular network of **4** with marked O–H $\cdots$ O and O–H $\cdots$ Cl hydrogen bonds (a); A view of the pairing of the chains showing the  $\pi$ – $\pi$  stacking between the pyridyl and thiophene rings of neighbouring 4'-R<sup>4</sup>-terpy ligands.

**Figure S3.** Experimental (black) and calculated (red) electronic absorption spectra of **1–6** in MeCN solution.

**Figure S4.** Natural transition orbitals (NTOs) of complexes **1–6** illustrating the nature of optically active singlet excited states in the absorption bands.

**Figure S5.** Excitation and emission spectra together with PL lifetime curves for **1–6** in CH<sub>2</sub>Cl<sub>2</sub>, CHCl<sub>3</sub>, MeCN and in solid state.

**Figure S6.** Isodensity surface plots of the HSOMO and LSOMO for the complexes **1–6** at their T<sub>1</sub> TDDFT state geometry. Blue and grey colours show regions of positive and negative spin density values, respectively.

**Figure S7.** X-ray diffraction patterns of blend with 15 % of **1**

**Figure S8.** AFM images (10  $\mu$ m x 10  $\mu$ m) of 15% doped PVK with (a) [ReCl(CO)<sub>3</sub>(4'-R<sup>1</sup>terpy- $\kappa$ <sup>2</sup>N)], (b) [ReCl(CO)<sub>3</sub>(4'-R<sup>4</sup>terpy- $\kappa$ <sup>2</sup>N)] (c) [ReCl(CO)<sub>3</sub>(4'-R<sup>6</sup>terpy- $\kappa$ <sup>2</sup>N)] and (d) pure PVK film in devices.

**Table S1.** Crystal data and structure refinement of **2**, **3** and **4** complexes.

	<b>2</b>	<b>3</b>	<b>4</b>
Empirical formula	C <sub>22</sub> H <sub>13</sub> ClN <sub>3</sub> O <sub>4</sub> Re	C <sub>22</sub> H <sub>13</sub> ClN <sub>3</sub> O <sub>3</sub> ReS	C <sub>26</sub> H <sub>19</sub> ClN <sub>3</sub> O <sub>5</sub> ReS <sub>2</sub>
Formula weight	605.00	621.06	739.24
Temperature [K]	298.0(2)	298.0(2)	298.0(2)
Wavelength [Å]	0.71073	0.71073	0.71073
Crystal system	monoclinic	monoclinic	monoclinic
Space group	P2 <sub>1</sub> /c	P2 <sub>1</sub> /c	P2 <sub>1</sub> /n
Unit cell dimensions [Å, °]	a = 11.6471(12) b = 11.1797(9) c = 15.9757(13) β = 103.161(9) 2025.6(3)	a = 11.4946(6) b = 11.4393(6) c = 16.3187(9) β = 103.256(5) 2088.58(19)	a = 15.0564(6) b = 7.5422(3) c = 24.6011(13) β = 105.250(5) 2695.3(2)
Volume [Å <sup>3</sup> ]			
Z	4	4	4
Density (calculated) [Mg/m <sup>3</sup> ]	1.984	1.975	1.822
Absorption coefficient [mm <sup>-1</sup> ]	6.167	6.076	4.805
F(000)	1160	1192	1440
Crystal size [mm]	0.34 x 0.27 x 0.04	0.10 x 0.10 x 0.03	0.29 x 0.04 x 0.03
θ range for data collection [°]	3.59 to 25.05	3.47 to 25.05	3.43 to 25.05
Index ranges	-13 ≤ h ≤ 11 -11 ≤ k ≤ 13 -18 ≤ l ≤ 19	-13 ≤ h ≤ 13 -13 ≤ k ≤ 13 -19 ≤ l ≤ 19	-17 ≤ h ≤ 17 -8 ≤ k ≤ 8 -26 ≤ l ≤ 29
Reflections collected	11467	10472	14216
Independent reflections	3578 (R <sub>int</sub> = 0.0671)	3700 (R <sub>int</sub> = 0.0443)	4742(R <sub>int</sub> = 0.050)
Completeness to 2θ=50° [%]	99.7	99.7	99.7
Max. and min. transmission	1.000 and 0.338	1.000 and 0.610	1.000 and 0.554
Data / restraints / parameters	3578 / 0 / 280	3700 / 0 / 280	4742 / 0 / 356
Goodness-of-fit on F <sup>2</sup>	1.047	1.062	1.079
Final R indices [I>2σ(I)]	R <sub>1</sub> = 0.0404 wR <sub>2</sub> = 0.0950	R <sub>1</sub> = 0.0344 wR <sub>2</sub> = 0.0792	R <sub>1</sub> = 0.0411 wR <sub>2</sub> = 0.0892
R indices (all data)	R <sub>1</sub> = 0.0556 wR <sub>2</sub> = 0.1048	R <sub>1</sub> = 0.0479 wR <sub>2</sub> = 0.0838	R <sub>1</sub> = 0.0566 wR <sub>2</sub> = 0.0964
Largest diff. peak and hole[e Å <sup>-3</sup> ]	1.695 and -1.597	1.286 and -1.237	1.150 and -0.753
CCDC number	1423469	1423470	1423471

**Table S2.** The experimental bond lengths [Å] and angles [°] for the rhenium(I) complexes.

	2	3	4
Bond lengths			
Re(1)–C(1)	1.925(10)	1.920(8)	1.932(9)
Re(1)–C(2)	1.898(9)	1.888(7)	1.912(7)
Re(1)–C(3)	1.946(10)	1.897(7)	1.918(8)
Re(1)–N(1)	2.157(6)	2.170(5)	2.172(5)
Re(1)–N(2)	2.209(5)	2.219(5)	2.224(5)
Re(1)–Cl(1)	2.483(2)	2.4828(16)	2.4927(16)
C(1)–O(1)	1.141(11)	1.153(8)	1.140(10)
C(2)–O(2)	1.150(10)	1.153(9)	1.136(8)
C(3)–O(3)	1.101(11)	1.148(8)	1.121(9)
Bond angles			
C(2)–Re(1)–C(1)	86.4(3)	86.8(3)	87.2(3)
C(3)–Re(1)–C(1)	88.2(3)	89.2(3)	91.4(3)
C(3)–Re(1)–C(2)	87.1(4)	86.4(3)	88.5(3)
C(1)–Re(1)–N(1)	174.9(3)	174.5(2)	175.3(2)
C(2)–Re(1)–N(1)	96.8(2)	96.8(2)	95.5(3)
C(3)–Re(1)–N(1)	95.9(3)	95.1(2)	92.6(3)
C(1)–Re(1)–N(2)	101.8(3)	101.8(2)	101.7(2)
C(2)–Re(1)–N(2)	171.2(3)	171.0(2)	168.6(2)
C(3)–Re(1)–N(2)	96.1(3)	96.3(2)	98.4(2)
N(1)–Re(1)–N(2)	74.77(19)	74.44(16)	75.24(19)
C(1)–Re(1)–Cl(1)	92.8(3)	92.4(2)	89.8(2)
C(2)–Re(1)–Cl(1)	93.3(3)	93.4(2)	91.9(2)
C(3)–Re(1)–Cl(1)	179.0(2)	178.4(2)	178.8(2)
N(1)–Re(1)–Cl(1)	83.10(16)	83.27(12)	86.25(13)
N(2)–Re(1)–Cl(1)	83.36(15)	83.61(12)	80.93(12)

**Table S3.** Short intra- and intermolecular contacts detected in the structures of the rhenium(I) complexes.

D—H···A	D—H	H···A	D···A [Å]	D—H···A [°]
<b>2</b>				
C(5)—H(5)···O(2)#1	0.93	2.56	3.208(11)	127.00
C(7)—H(7)···Cl(1)#2	0.93	2.66	3.567(8)	166.00
C(12)—H(12)···O(4)	0.93	2.49	2.806(9)	100.00
<b>3</b>				
C(5)—H(5)···O(2)#3	0.93	2.58	3.232(8)	127.00
C(7)—H(7)···Cl(1)#4	0.93	2.65	3.559(7)	165.00
C(12)—H(12)···S(1)	0.93	2.71	3.108(6)	107.00
<b>4</b>				
O(5B)—H(5BA)···O(4)#5	0.85	1.86	2.644(19)	152.00
O(5B)—H(5BB)···Cl(1)#5	0.85	2.48	3.21(2)	145.00
O(4)—H(4A)···O(5B)	0.85	1.90	2.68(2)	152.00
O(4)—H(4B)···N(3)	0.85	2.14	2.967(13)	163.00
C(7)—H(7)···Cl(1)#6	0.93	2.80	3.680(7)	159.00
C(12)—H(12)···S(1)	0.93	2.73	3.119(7)	106.00
C(16)—H(16)···O(3)#7	0.93	2.41	3.339(12)	175.00
C(20)—H(20)···Cl(1)#6	0.93	2.74	3.569(7)	150.00

Symmetry codes: #1: -x,-y,-z; #2: 1-x,-1/2+y,1/2-z; #3: 1-x,1-y,-z; #4: 2-x,1/2+y,1/2-z; #5: 3/2-x,-1/2+y,3/2-z  
#6: 1-x,2-y,1-z; #7: 2-x,1-y,1-z

**Table S4.** Comparison of experimental and theoretical bond lengths [Å] and angles [°] for **2**, **3** and **4**.

Bond lengths	Exp.	Opt.	Bond angles	Exp.	Opt.
		S <sub>0</sub>			S <sub>0</sub>
<b>2</b>					
Re(1)–C(1)	1.925(10)	1.913	C(2)–Re(1)–C(1)	86.4(3)	91.13
Re(1)–C(2)	1.898(9)	1.939	C(3)–Re(1)–C(1)	88.2(3)	89.87
Re(1)–C(3)	1.946(10)	1.921	C(3)–Re(1)–C(2)	87.1(4)	86.98
Re(1)–N(1)	2.157(6)	2.202	C(1)–Re(1)–N(1)	174.9(3)	93.10
Re(1)–N(2)	2.209(5)	2.266	C(2)–Re(1)–N(1)	96.8(2)	174.40
Re(1)–Cl(1)	2.483(2)	2.550	C(3)–Re(1)–N(1)	95.9(3)	96.69
C(1)–O(1)	1.141(11)	1.170	C(1)–Re(1)–N(2)	101.8(3)	96.34
C(2)–O(2)	1.150(10)	1.164	C(2)–Re(1)–N(2)	171.2(3)	101.61
C(3)–O(3)	1.101(11)	1.169	C(3)–Re(1)–N(2)	96.1(3)	169.25
			N(1)–Re(1)–N(2)	74.77(19)	74.28
			C(1)–Re(1)–Cl(1)	92.8(3)	177.74
			C(2)–Re(1)–Cl(1)	93.3(3)	90.95
			C(3)–Re(1)–Cl(1)	179.0(2)	91.13
			N(1)–Re(1)–Cl(1)	83.10(16)	84.77
			N(2)–Re(1)–Cl(1)	83.36(15)	82.38
<b>3</b>					
Re(1)–C(1)	1.920(8)	1.919	C(2)–Re(1)–C(1)	86.8(3)	86.84
Re(1)–C(2)	1.888(7)	1.937	C(3)–Re(1)–C(1)	89.2(3)	90.23
Re(1)–C(3)	1.897(7)	1.915	C(3)–Re(1)–C(2)	86.4(3)	90.60
Re(1)–N(1)	2.170(5)	2.202	C(1)–Re(1)–N(1)	174.5(2)	169.31
Re(1)–N(2)	2.219(5)	2.262	C(2)–Re(1)–N(1)	96.8(2)	96.32
Re(1)–Cl(1)	2.4828(16)	2.554	C(3)–Re(1)–N(1)	95.1(2)	93.52
C(1)–O(1)	1.153(8)	1.168	C(1)–Re(1)–N(2)	101.8(2)	102.22
C(2)–O(2)	1.153(9)	1.164	C(2)–Re(1)–N(2)	171.0(2)	169.31
C(3)–O(3)	1.148(8)	1.169	C(3)–Re(1)–N(2)	96.3(2)	95.27
			N(1)–Re(1)–N(2)	74.44(16)	74.24
			C(1)–Re(1)–Cl(1)	92.4(2)	91.66
			C(2)–Re(1)–Cl(1)	93.4(2)	91.05
			C(3)–Re(1)–Cl(1)	178.4(2)	177.55
			N(1)–Re(1)–Cl(1)	83.27(12)	84.73
			N(2)–Re(1)–Cl(1)	83.61(12)	82.61
<b>4</b>					
Re(1)–C(1)	1.932(9)	1.939	C(2)–Re(1)–C(1)	87.2(3)	91.17
Re(1)–C(2)	1.912(7)	1.913	C(3)–Re(1)–C(1)	91.4(3)	86.96
Re(1)–C(3)	1.918(8)	1.921	C(3)–Re(1)–C(2)	88.5(3)	89.83
Re(1)–N(1)	2.172(5)	2.203	C(1)–Re(1)–N(1)	175.3(2)	174.34
Re(1)–N(2)	2.224(5)	2.264	C(2)–Re(1)–N(1)	95.5(3)	93.16
Re(1)–Cl(1)	2.4927(16)	2.550	C(3)–Re(1)–N(1)	92.6(3)	96.69
C(1)–O(1)	1.140(10)	1.170	C(1)–Re(1)–N(2)	101.7(2)	101.68
C(2)–O(2)	1.136(8)	1.164	C(2)–Re(1)–N(2)	168.6(2)	169.30
C(3)–O(3)	1.121(9)	1.167	C(3)–Re(1)–N(2)	98.4(2)	96.23
			N(1)–Re(1)–N(2)	75.24(19)	74.24
			C(1)–Re(1)–Cl(1)	89.8(2)	90.92
			C(2)–Re(1)–Cl(1)	91.9(2)	91.14
			C(3)–Re(1)–Cl(1)	178.8(2)	177.74
			N(1)–Re(1)–Cl(1)	86.25(13)	84.70
			N(2)–Re(1)–Cl(1)	80.93(12)	82.50

**Table S5.** Frontier molecular orbital composition (%) in the ground state for complex **1** calculated at the DFT/B3LYP/DEF2-TZVPD level.

Orbital	Energy [eV]	Contribution (%)					Character
		Re	3CO	Cl	R	terpy	
LUMO+5	-0.78	17.85	24.33	2.89	0.09	54.84	$\pi^*(4'-R\text{-terpy}) + d(Re) + \pi^*(CO)$
LUMO+4	-1.00	21.61	36.74	8.46	0.17	33.02	$d(Re) + \pi^*(CO) + \pi^*(4'-R\text{-terpy})$
LUMO+3	-1.19	23.04	19.04	0.81	1.57	55.54	$\pi^*(4'-R\text{-terpy}) + d(Re) + \pi^*(CO)$
LUMO+2	-1.50	12.53	4.77	1.83	1.44	79.43	$\pi^*(4'-R\text{-terpy}) + d(Re)$
LUMO+1	-1.87	4.88	1.65	0.89	8.12	84.46	$\pi^*(4'-R\text{-terpy})$
LUMO	-2.53	10.25	3.74	2.77	6.59	76.65	$\pi^*(4'-R\text{-terpy}) + d(Re)$
HOMO	-5.94	10.51	4.68	1.85	59.86	23.10	$\pi(4'-R\text{-terpy}) + d(Re)$
HOMO-1	-6.30	43.76	26.08	22.67	0.89	6.60	$d(Re) + \pi(CO) + p(Cl)$
HOMO-2	-6.47	36.01	21.79	26.14	8.05	8.01	$d(Re) + \pi(CO) + p(Cl)$
HOMO-3	-6.73	54.66	31.22	1.49	0.10	12.53	$d(Re) + \pi(CO)$
HOMO-4	-6.86	0.26	0.02	0.10	97.25	2.37	$\pi(4'-R\text{-terpy})$
HOMO-5	-7.08	2.95	2.72	0.24	0.81	93.28	$\pi(4'-R\text{-terpy})$

**Table S6.** Frontier molecular orbital composition (%) in the ground state for complex **2** calculated at the DFT/B3LYP/DEF2-TZVPD level.

Orbital	Energy [eV]	Contribution (%)					Character
		Re	3CO	Cl	R	terpy	
LUMO+5	-0.844	17.48	22.40	0.65	11.35	48.12	$\pi^*(4'-R\text{-terpy}) + d(Re) + \pi^*(CO)$
LUMO+4	-1.007	21.06	36.41	8.49	0.10	33.94	$d(Re) + \pi^*(CO) + \pi^*(4'-R\text{-terpy})$
LUMO+3	-1.236	19.91	17.14	0.69	2.33	59.93	$\pi^*(4'-R\text{-terpy}) + d(Re) + \pi^*(CO)$
LUMO+2	-1.549	13.59	4.98	2.06	1.72	77.65	$\pi^*(4'-R\text{-terpy}) + d(Re)$
LUMO+1	-1.977	2.63	1.77	0.65	7.88	87.07	$\pi^*(4'-R\text{-terpy})$
LUMO	-2.656	9.95	3.44	2.71	9.67	74.23	$\pi^*(4'-R\text{-terpy})$
HOMO	-6.252	30.31	18.08	11.69	25.60	14.32	$d(Re) + \pi(CO) + p(Cl) + \pi(4'-R\text{-terpy})$
HOMO-1	-6.332	41.79	22.68	20.21	6.32	9.00	$d(Re) + \pi(CO) + p(Cl)$
HOMO-2	-6.614	17.27	10.59	19.96	16.72	35.46	$\pi(4'-R\text{-terpy}) + d(Re) + \pi(CO) + p(Cl)$
HOMO-3	-6.754	54.35	30.88	1.56	12.16	1.05	$d(Re) + \pi(CO)$
HOMO-4	-6.748	2.98	2.76	0.48	0.72	93.06	$\pi(4'-R\text{-terpy})$
HOMO-5	-7.129	2.14	1.07	7.13	0.46	89.20	$\pi(4'-R\text{-terpy})$

**Table S7.** Frontier molecular orbital composition (%) in the ground state for complex **3** calculated at the DFT/B3LYP/DEF2-TZVPD level.

Orbital	Energy [eV]	Contribution (%)					Character
		Re	3CO	Cl	R	terpy	
LUMO+5	-0.926	31.39	34.44	6.39	6.67	21.12	$d(Re) + \pi^*(CO) + \pi^*(4'-R\text{-terpy})$
LUMO+4	-1.034	22.91	23.09	2.57	0.73	50.70	$\pi^*(4'-R\text{-terpy}) + d(Re) + \pi^*(CO)$
LUMO+3	-1.213	10.44	7.07	0.70	9.08	72.71	$\pi^*(4'-R\text{-terpy}) + d(Re)$
LUMO+2	-1.542	9.42	4.40	1.95	3.12	81.11	$\pi^*(4'-R\text{-terpy})$
LUMO+1	-1.994	1.29	1.33	0.42	13.34	83.62	$\pi^*(4'-R\text{-terpy})$
LUMO	-2.686	10.28	3.27	2.85	12.03	71.56	$\pi^*(4'-R\text{-terpy}) + d(Re)$
HOMO	-6.229	41.24	25.60	19.22	5.77	8.17	$d(Re) + \pi(CO) + p(Cl)$
HOMO-1	-6.312	38.85	21.36	17.15	11.57	11.07	$d(Re) + \pi(CO) + p(Cl) + \pi(4'-R\text{-terpy})$
HOMO-2	-6.675	14.28	8.38	14.21	45.03	18.09	$\pi(4'-R\text{-terpy}) + d(Re) + \pi(CO) + p(Cl)$
HOMO-3	-6.716	51.48	28.87	1.96	6.70	10.98	$d(Re) + \pi(CO) + p(Cl) + \pi(4'-R\text{-terpy})$
HOMO-4	-7.129	0.99	1.28	0.26	11.80	85.67	$\pi(4'-R\text{-terpy})$
HOMO-5	-7.320	0.15	0.16	0.11	89.67	9.91	$\pi(4'-R\text{-terpy})$

**Table S8.** Frontier molecular orbital composition (%) in the ground state for complex **4** calculated at the DFT/B3LYP/DEF2-TZVPD level.

Orbital	Energy [eV]	Contribution (%)					Character
		Re	3CO	Cl	R	terpy	
LUMO+5	-1.007	23.36	37.46	8.32	0.18	30.68	$d(Re) + \pi^*(CO) + \pi^*(4'-R-terpy)$
LUMO+4	-1.143	27.29	21.78	0.86	10.37	39.70	$\pi^*(4'-R-terpy) + d(Re) + \pi^*(CO)$
LUMO+3	-1.213	4.42	15.83	0.26	21.33	58.17	$\pi^*(4'-R-terpy)$
LUMO+2	-1.542	11.98	15.19	2.28	12.46	58.08	$\pi^*(4'-R-terpy) + d(Re) + \pi^*(CO)$
LUMO+1	-1.994	2.30	2.36	0.60	20.04	74.40	$\pi^*(4'-R-terpy)$
LUMO	-2.686	8.66	3.36	2.30	22.68	63.00	$\pi^*(4'-R-terpy)$
HOMO	-6.229	6.14	2.15	0.81	76.92	13.98	$\pi(4'-R-terpy)$
HOMO-1	-6.312	43.69	26.96	22.87	0.60	5.88	$d(Re) + \pi(CO) + p(Cl)$
HOMO-2	-6.675	39.83	24.08	25.14	4.74	6.21	$d(Re) + \pi(CO) + p(Cl)$
HOMO-3	-6.716	54.47	31.86	1.55	0.13	11.99	$d(Re) + \pi(CO)$
HOMO-4	-7.102	2.47	6.41	0.06	18.57	72.49	$\pi(4'-R-terpy)$
HOMO-5	-7.184	0.24	0.66	0.01	91.35	7.74	$\pi(4'-R-terpy)$

**Table S9.** Frontier molecular orbital composition (%) in the ground state for complex **5** calculated at the DFT/B3LYP/DEF2-TZVPD level.

Orbital	Energy [eV]	Contribution (%)					Character
		Re	3CO	Cl	R	terpy	
LUMO+5	-0.95	31.33	34.38	5.19	7.12	21.98	$d(Re) + \pi^*(CO) + \pi^*(4'-R-terpy)$
LUMO+4	-1.03	21.17	22.07	3.05	1.00	52.71	$\pi^*(4'-R-terpy) + d(Re) + \pi^*(CO)$
LUMO+3	-1.25	9.88	5.38	0.51	10.58	73.65	$\pi^*(4'-R-terpy) + d(Re)$
LUMO+2	-1.55	9.12	4.36	2.04	3.61	80.87	$\pi^*(4'-R-terpy)$
LUMO+1	-2.06	1.39	1.39	0.39	14.81	82.02	$\pi^*(4'-R-terpy)$
LUMO	-2.74	10.77	3.10	2.80	13.94	69.39	$\pi^*(4'-R-terpy) + d(Re)$
HOMO	-6.17	17.79	10.76	6.29	54.20	10.96	$\pi(4'-R-terpy) + d(Re) + \pi^*(CO)$
HOMO-1	-6.26	39.42	23.01	19.39	11.06	7.12	$d(Re) + \pi(CO) + p(Cl) + \pi(4'-R-terpy)$
HOMO-2	-6.42	27.34	15.92	16.24	35.84	4.66	$d(Re) + \pi(CO) + p(Cl) + \pi(4'-R-terpy)$
HOMO-3	-6.67	8.07	4.76	7.69	68.40	11.08	$\pi(4'-R-terpy)$
HOMO-4	-6.55	53.21	29.82	1.34	5.97	9.66	$d(Re) + \pi(CO)$
HOMO-5	-7.17	1.05	1.44	0.27	1.12	96.12	$\pi(4'-R-terpy)$

**Table S10.** Frontier molecular orbital composition (%) in the ground state for complex **6** calculated at the DFT/B3LYP/DEF2-TZVPD level.

Orbital	Energy [eV]	Contribution (%)					Character
		Re	3CO	Cl	R	terpy	
LUMO+5	-0.90	31.09	34.84	6.81	6.13	21.13	$d(Re) + \pi^*(CO) + \pi^*(4'-R-terpy)$
LUMO+4	-1.01	24.03	23.46	2.47	0.80	49.24	$\pi^*(4'-R-terpy) + d(Re) + \pi^*(CO)$
LUMO+3	-1.18	9.76	7.90	0.79	7.87	73.68	$\pi^*(4'-R-terpy)$
LUMO+2	-1.51	9.60	4.30	1.93	2.73	81.44	$\pi^*(4'-R-terpy)$
LUMO+1	-1.96	1.28	1.38	0.38	15.42	81.54	$\pi^*(4'-R-terpy)$
LUMO	-2.64	9.04	3.27	2.79	15.11	69.79	$\pi^*(4'-R-terpy)$
HOMO	-5.78	6.69	2.63	0.91	74.61	15.16	$\pi(4'-R-terpy)$
HOMO-1	-6.23	44.00	26.42	21.64	1.06	6.88	$d(Re) + \pi(CO) + p(Cl)$
HOMO-2	-6.40	38.71	23.12	24.13	7.47	6.57	$d(Re) + \pi(CO) + p(Cl) + \pi(4'-R-terpy)$
HOMO-3	-6.69	56.58	32.08	1.54	0.10	9.70	$d(Re) + \pi(CO)$
HOMO-4	-7.02	0.87	0.38	1.56	77.11	20.08	$\pi(4'-R-terpy)$
HOMO-5	-7.15	0.98	1.16	0.67	21.34	75.85	$\pi(4'-R-terpy)$

**Table S11.** The energies and characters of the selected spin-allowed electronic transitions for **1** calculated with the TDDFT/B3LYP method, together with assignment to the experimental absorption bands.

Experimental absorption $\lambda$ ; nm ( $10^{-3} \epsilon$ ; M <sup>-1</sup> cm <sup>-1</sup> )	Calculated transitions				
	Major contribution (%)	Character	E [eV]	$\lambda$ [nm]	Oscillator strength
383.8 (22.2)	H → L	ILCT/IL	2.94	421.63	0.2243
	H-1 → L	MLCT/LLCT	3.06	405.25	0.1049
351.9 (21.1)	H → L+1	ILCT/IL	3.51	353.63	0.2326
301.3 (31.4)	H-2 → L+1	MLCT/LLCT	3.95	314.14	0.0952
	H-5 → L	IL	3.97	312.32	0.1282
	H-1 → L+2	MLCT/LLCT/LF	4.06	305.14	0.1010
253.3 (28.6)	H → L+6	ILCT/LMCT/IL	4.68	264.74	0.1502
	H-9 → L	LLCT/IL	4.75	260.80	0.1119
	H → L+6	ILCT/LMCT/IL	4.79	259.04	0.0757
	H-7 → L+1	IL	5.11	242.53	0.0652
221.9 (37.8)	H-6 → L+2	IL	5.50	225.12	0.0597
	H → L+7	LLCT/IL			
	H-5 → L+7	LLCT/IL	6.24	198.60	0.0529

**Table S12.** The energies and characters of the selected spin-allowed electronic transitions for **2** calculated with the TDDFT/B3LYP method, together with assignment to the experimental absorption bands.

Experimental absorption $\lambda$ ; nm ( $10^{-3} \epsilon$ ; M <sup>-1</sup> cm <sup>-1</sup> )	Calculated transitions				
	Major contribution (%)	Character	E [eV]	$\lambda$ [nm]	Oscillator strength
383.2 (22.0)	H → L	MLCT/LLCT/ILCT/IL	2.93	423.6	0.0200
	H-1 → L	MLCT/LLCT	3.06	404.6	0.1939
	H-3 → L	MLCT/LLCT	2.35	370.5	0.0109
340.2(26.8)	H-2 → L	MLCT/LLCT/IL	3.50	354.7	0.1815
	H → L+1	MLCT/LLCT/ILCT/IL	3.66	338.9	0.1276
304.2 (32.6)	H-4 → L	IL	3.89	319.0	0.1655
	H → L+2	MLCT/LLCT/IL/LF	4.01	309.2	0.0639
	H-1 → L+2	MLCT/LLCT	4.02	308.2	0.1086
	H-2 → L+1	MLCT/LLCT/IL	4.08	303.8	0.1985
253.1 (27.4)	H-2 → L+2	MLCT/LLCT/IL/LF	4.53	273.4	0.0628
	H-3 → L+3	MLCT/LLCT	4.67	265.5	0.0791
	H-4 → L+1	IL	4.72	262.7	0.0736
	H-2 → L+3	MLCT/LLCT/IL/LF	4.75	261.1	0.1004
	H-9 → L	IL	5.05	245.7	0.0632
198.0 (60.9)	H-10 → L+1 H-4 → L+6	ILCT IL/LMCT/LLCT	5.53	223.9	0.0584
	H-3 → L+8	IL/d-d	5.71	217.3	0.0598
	H-11 → L+2	LLCT	6.30	196.8	0.0569
	H-10 → L+4	IL/LMCT	6.57	188.8	0.0504
	H → L+15	ILCT/ LMCT	6.60	187.2	0.0526
	H-5 → L+8	ILCT/ LMCT	6.65	186.4	0.0577
	H-15 → L+1	IL	6.85	180.9	0.0919

$\epsilon$  – molar absorption coefficient; H – highest occupied molecular orbital; L – lowest unoccupied molecular orbital

**Table S13.** The energies and characters of the selected spin-allowed electronic transitions for **3** calculated with the TDDFT/B3LYP method, together with assignment to the experimental absorption bands.

Experimental absorption $\lambda$ ; nm ( $10^{-3} \epsilon$ ; M <sup>-1</sup> cm <sup>-1</sup> )	Calculated transitions				
	Major contribution (%)	Character	E [eV]	$\lambda$ [nm]	Oscillator strength
381.0 (4.4)	H-1 → L	MLCT/LLCT	3.02	410.9	0.1763
321.2 (13.2)	H-2 → L	ILCT/MLCT/LLCT/IL	3.53	351.3	0.2253
	H → L+1	MLCT/LLCT	3.60	344.6	0.0900
	H-1 → L+1	MLCT/LLCT/ILCT/IL	3.69	335.9	0.0502
	H-2 → L	ILCT/MLCT/LLCT/IL	3.87	320.1	0.1135
	H → L+2	MLCT/LLCT	3.99	311.1	0.0546
	H-5 → L	ILCT	4.11	301.7	0.1090
	H-2 → L+1	ILCT/MLCT/LLCT/IL	4.15	298.9	0.2070
	H-5 → L	ILCT			
258.3 (12.7)	H-2 → L+2	ILCT/MLCT/LLCT/IL	4.63	267.8	0.0659
	H-4 → L+1	IL	4.68	264.8	0.0778
	H-3 → L+4	LMCT/LLCT/LF	4.76	260.6	0.0697
193.7 (149.2)	H-4 → L+3	IL	5.33	232.8	0.0891
	H-8 → L+2	LLCT/IL	5.65	219.5	0.0740
	H-5 → L+3	ILCT/IL			
	H-4 → L+6	IL/LLCT	5.86	211.6	0.0472
	H-11 → L+2	LLCT	6.28	197.4	0.0557
	H-9 → L+6	LLCT/IL	6.44	192.4	0.0714

$\epsilon$  – molar absorption coefficient; H – highest occupied molecular orbital; L – lowest unoccupied molecular orbital

**Table S14.** The energies and characters of the selected spin-allowed electronic transitions for **4** calculated with the TDDFT/B3LYP method, together with assignment to the experimental absorption bands.

Experimental absorption $\lambda$ ; nm ( $10^{-3} \epsilon$ ; M <sup>-1</sup> cm <sup>-1</sup> )	Calculated transitions				
	Major contribution (%)	Character	E [eV]	$\lambda$ [nm]	Oscillator strength
406.3 (19.8)	H → L	ILCT/IL	2.69	459.6	0.8277
	H-1 → L	MLCT/LLCT	2.88	429.6	0.0372
	H → L+1	ILCT/IL	3.28	377.9	0.2479
313.7 (14.9)	H-2 → L+1	MLCT/LLCT	3.74	330.8	0.0541
	H-4 → L	ILCT/IL	3.75	330.6	0.1390
	H-2 → L+1	MLCT/LLCT/ILCT/IL			
	H-4 → L	IL/ILCT	3.83	323.0	0.0872
	H-1 → L+2	MLCT/LLCT/LMCT/LF	4.00	309.8	0.0626
	H → L+3	ILCT/IL	4.01	308.6	0.0608
257.4 (16.3)	H-2 → L+5	MLCT/LLCT/IL/ILCT	4.58	270.4	0.0921
	H-3 → L+3	MLCT/LLCT	4.70	263.4	0.0889
	H-3 → L+4	MLCT/LLCT/LF			
	H-6 → L+1	ILCT/IL	4.84	255.9	0.0561
	H-13 → L	LLCT	5.12	241.9	0.0532
	H-4 → L+3	ILCT/IL	5.20	238.4	0.0884
219.7 (23.7)	H-14 → L	IL	5.48	226.2	0.0842
	H-6 → L+3	ILCT/IL	5.53	223.8	0.0450
	H-10 → L+2	LLCT/LMCT/IL	5.58	221.9	0.0461
	H-4 → L+9	IL/LMCT	6.43	192.8	0.0501

$\epsilon$  – molar absorption coefficient; H – highest occupied molecular orbital; L – lowest unoccupied molecular orbital

**Table S15.** The energies and characters of the selected spin-allowed electronic transitions for **5** calculated with the TDDFT/B3LYP method, together with assignment to the experimental absorption bands.

Experimental absorption $\lambda$ ; nm ( $10^{-3} \epsilon$ ; M <sup>-1</sup> cm <sup>-1</sup> )	Calculated transitions				
	Major contribution (%)	Character	E [eV]	$\lambda$ [nm]	Oscillator strength
383.2 (22)	H-1 → L	MLCT/LLCT/ILCT/IL	2.80	442.8	0.0217
	H → L	ILCT /IL/MLCT/LLCT			
	H → L	ILCT /IL/MLCT/LLCT	2.95	419.80	0.3383
340.2(26.8)	H-2 → L	MLCT/LLCT/ILCT/IL	3.14	394.01	0.0563
	H-3 → L	ILCT/IL	3.45	359.25	0.3002
304.2 (32.6)	H → L+1	ILCT /IL/MLCT/LLCT	3.52	351.45	0.0914
	H-5 → L	IL	3.85	321.54	0.1367
	H-1 → L+2	MLCT/LLCT/ILCT/IL	3.97	311.67	0.0641
	H-3 → L+1	ILCT/IL	4.10	301.92	0.1921
253.1 (27.4)	H-2 → L+2	MLCT/LLCT/ILCT/IL	4.35	285.00	0.0824
	H-1 → L+3	MLCT/LLCT/ILCT/IL	4.55	272.49	0.0593
	H-2 → L+3	MLCT/LLCT/ILCT/IL	4.65	266.59	0.0631
	H-5 → L+1	IL	4.66	265.74	0.0799
221.8 (38.7)	H-7 → L+1	IL	4.93	251.02	0.0856
	H-4 → L+6	MLCT//LLCT	5.19	238.59	0.0717
	H-5 → L+3	IL	5.31	233.40	0.0889
	H-10 → L+1	ILCT/IL	5.52	224.56	0.0586
	H-9 → L+2	LLCT/IL	5.64	219.59	0.0513
198.0 (80)	H-2 → L+7	MLCT/LLCT/ILCT/IL	5.72	216.62	0.0796
	H-5 → L+6	IL/LLCT	5.85	211.80	0.0550
	H-3 → L+8	ILCT/LLCT/IL	5.98	207.11	0.1238
	H-3 → L+8	ILCT/LLCT/IL	6.34	195.39	0.0638

$\epsilon$  – molar absorption coefficient; H – highest occupied molecular orbital; L – lowest unoccupied molecular orbital

**Table S16.** The energies and characters of the selected spin-allowed electronic transitions for **6** calculated with the TDDFT/B3LYP method, together with assignment to the experimental absorption bands

Experimental absorption $\lambda$ ; nm ( $10^{-3} \epsilon$ ; M <sup>-1</sup> cm <sup>-1</sup> )	Calculated transitions				
	Major contribution (%)	Character	E [eV]	$\lambda$ [nm]	Oscillator strength
386.9 (9.0)	H → L	ILCT/IL	2.76	448.72	0.4151
	H-1 → L	MLCT/LLCT	2.91	426.80	0.0745
341.0 (12.0)	H → L+1	ILCT/IL	3.34	371.34	0.2875
	H-2 → L+1	MLCT/LLCT/IL	3.82	324.48	0.0541
305.2 (15.2)	H-4 → L	ILCT/IL	3.86	320.93	0.1693
	H-1 → L+2	MLCT/LLCT	4.03	307.62	0.1339
255.3 (12.5)	H-5 → L+1	IL/ILCT	4.74	261.56	0.0800
221.5 (18.8)	H-4 → L+3	ILCT/IL	5.32	233.06	0.0911
	H-5 → L+3	IL/ILCT			

$\epsilon$  – molar absorption coefficient; H – highest occupied molecular orbital; L – lowest unoccupied molecular orbital

**Table S17.** The energies and characters of the two lowest vertical electronic transitions for **4** complex obtained in TDDFT calculations with using different functionals.<sup>a</sup>

State	E [eV]	$\lambda$ [nm]	$f$	%	Character		
B3LYP							
S <sub>1</sub>	2.70	459.6	0.8281	96	140 → 141 H → L	$\pi_{R/\text{terpy}} \rightarrow \pi^*_{\text{terpy}/R}$	ILCT
S <sub>2</sub>	2.89	429.6	0.0372	96	139 → 141 H-1 → L	d → $\pi^*_{\text{terpy}/R}$	MLCT
BP86							
S <sub>1</sub>	2.08	595.7	0.4417	85	140 → 141 H → L	$\pi_{R/\text{terpy}} \rightarrow \pi^*_{\text{terpy}/R}$	ILCT
S <sub>2</sub>	2.20	564.7	0.0171	98	139 → 141 H-1 → L	d → $\pi^*_{\text{terpy}/R}$	MLCT
$\omega$ B97							
S <sub>1</sub>	3.92	316.6	1.2055	68	140 → 141 H → L	$\pi_{R/\text{Tterpy}} \rightarrow \pi^*_{\text{terpy}/R}$	ILCT
S <sub>2</sub>	4.13	300.3	0.0274	41	139 → 141 H-1 → L	d → $\pi^*_{\text{terpy}/R}$	MLCT
				21	139 → 146 H-1 → L +6	d → $\pi^*_{\text{terpy}/CO}$	MLCT
$\omega$ B97x							
S <sub>1</sub>	3.79	326.9	1.2066	70	140 → 141 H → L	$\pi_{R/\text{terpy}} \rightarrow \pi^*_{\text{terpy}/R}$	ILCT
				10	140 → 142 H → L+2	$\pi_{R/\text{terpy}} \rightarrow \pi^*_{\text{terpy}}$	ILCT
S <sub>2</sub>	4.02	308.1	0.0340	57	139 → 141 H-1 → L	d → $\pi^*_{\text{terpy}/R}$	MLCT
				14	139 → 146 H-1 → L +6	d → $\pi^*_{\text{TP}/CO}$	MLCT
CAM-B3LYP							
S <sub>1</sub>	3.43	361.2	1.1193	81	140 → 141 H → L	$\pi_R \rightarrow \pi^*_{\text{terpy}/R}$	ILCT
S <sub>2</sub>	3.64	340.4	0.0585	83	139 → 141 H-1 → L	d → $\pi^*_{\text{terpy}/R}$	MLCT
LC-BLYP							
S <sub>1</sub>	4.00	310.3	1.1841	67	140 → 141 H → L	$\pi_R \rightarrow \pi^*_{\text{terpy}/R}$	ILCT
				10	140 → 142 H → L+2	$\pi_R \rightarrow \pi^*_{\text{terpy}}$	ILCT
S <sub>2</sub>	4.19	295.6	0.0463	42	139 → 141 H-1 → L	d → $\pi^*_{\text{terpy}/R}$	MLCT
				20	139 → 146 H-1 → L +6	d → $\pi^*_{\text{terpy}/CO}$	MLCT

<sup>a)</sup> B3LYP - Becke, 3-parameter, Lee-Yang-Parr hybrid GGA exchange-correlation functional, BP86 -Becke 1988, Perdew 86 gradient-corrected exchange-correlation functional,  $\omega$ B97 – long range corrected Becke 1997 GGA exchange-correlation functional,  $\omega$ B97x – long range corrected hybrid Becke 1997 GGA exchange-correlation functional, CAM-B3LYP - long range corrected B3LYP functional, LC-BLYP - long range corrected Becke's 1988 exchange functional with the correlation functional by Lee, Yang, and Parr.

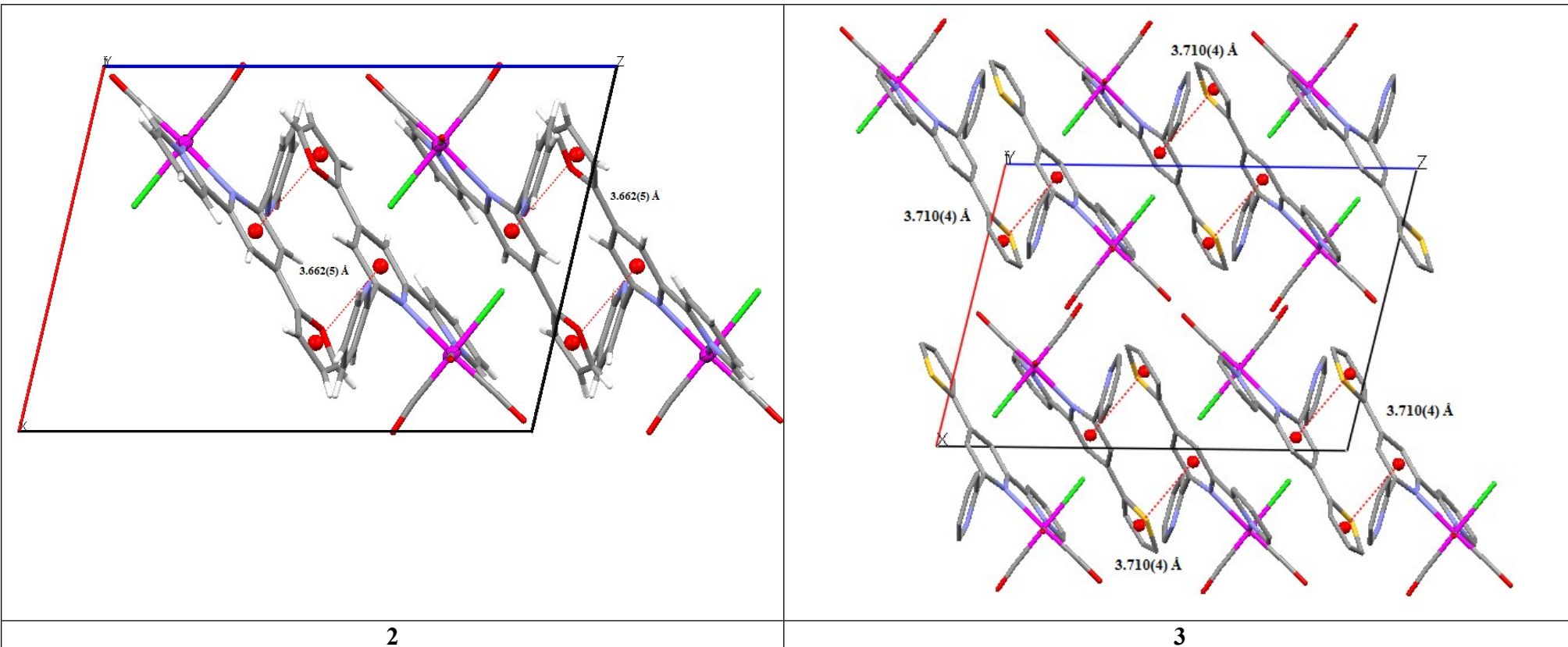


**Figure S1.** A view of the crystal packing showing intermolecular  $\pi$ - $\pi$  stacking interactions for **2** and **3**.

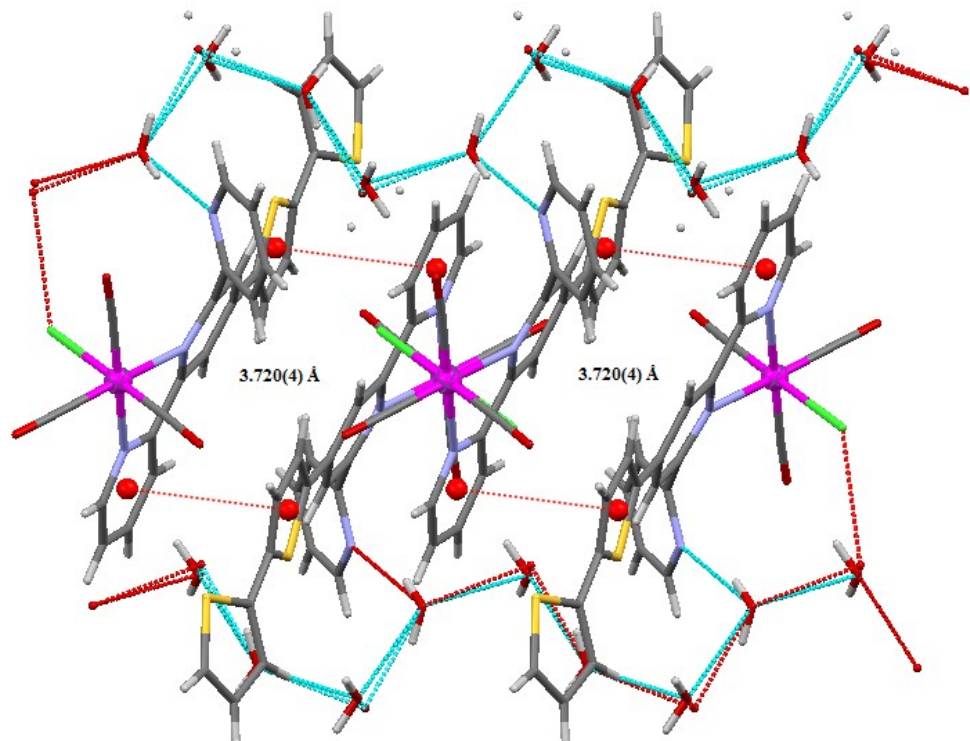
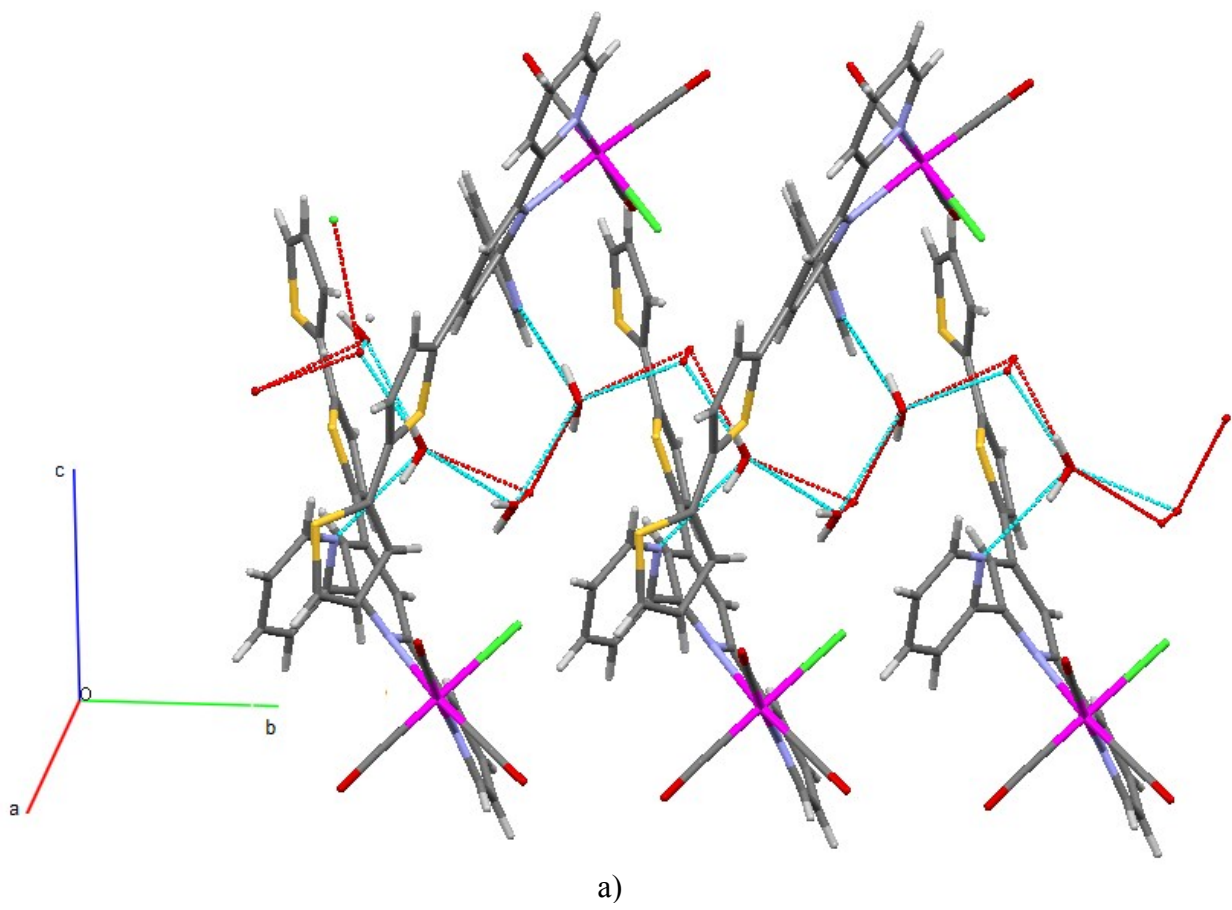


**Figure S2.** 1D supramolecular network of **4** with marked O–H $\cdots$ O and O–H $\cdots$ Cl hydrogen bonds (a); A view of the pairing of the chains showing the  $\pi$ – $\pi$  stacking between the pyridyl and thiophene rings of neighbouring 4'-R<sup>4</sup>-terpy ligands.

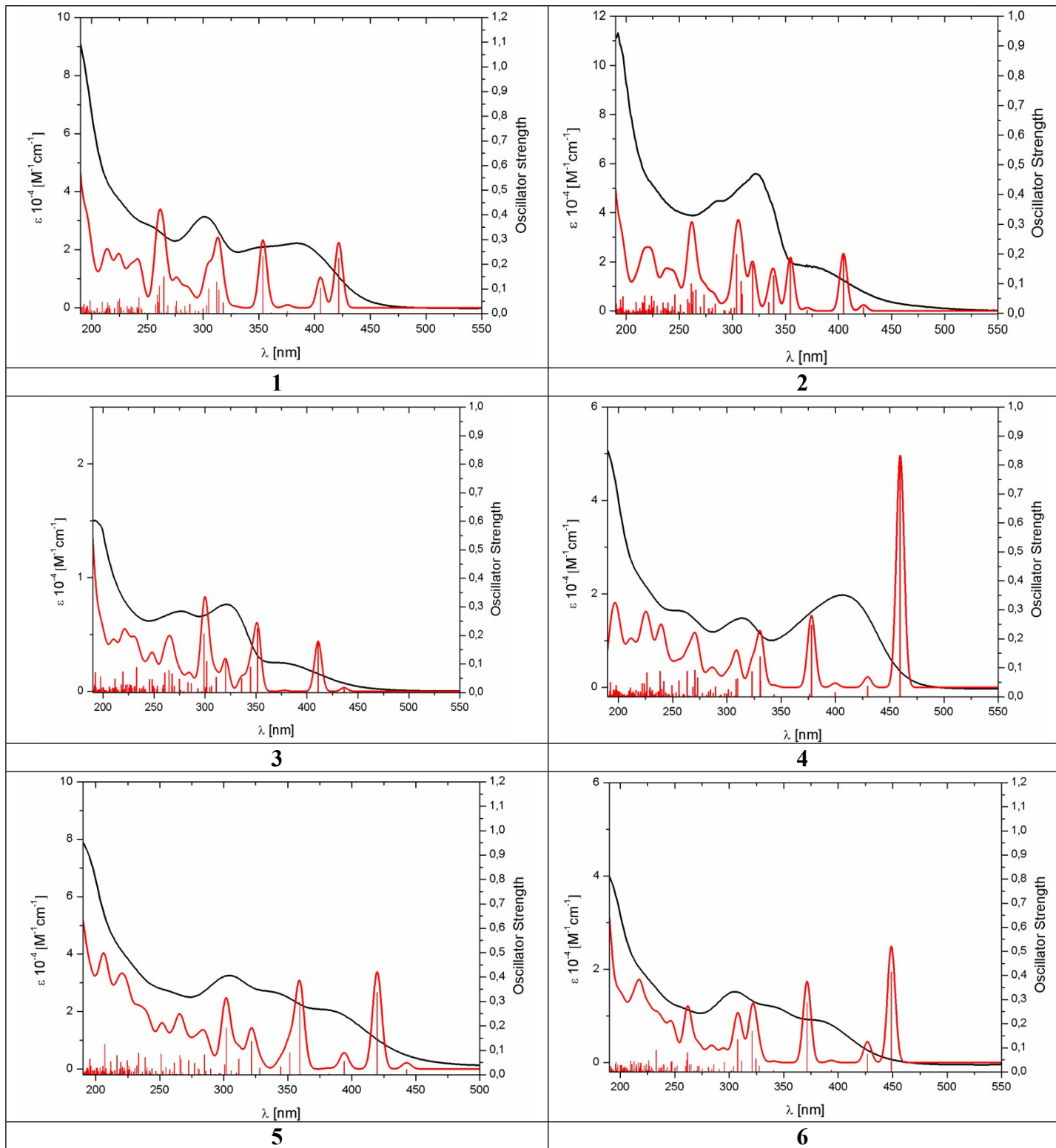


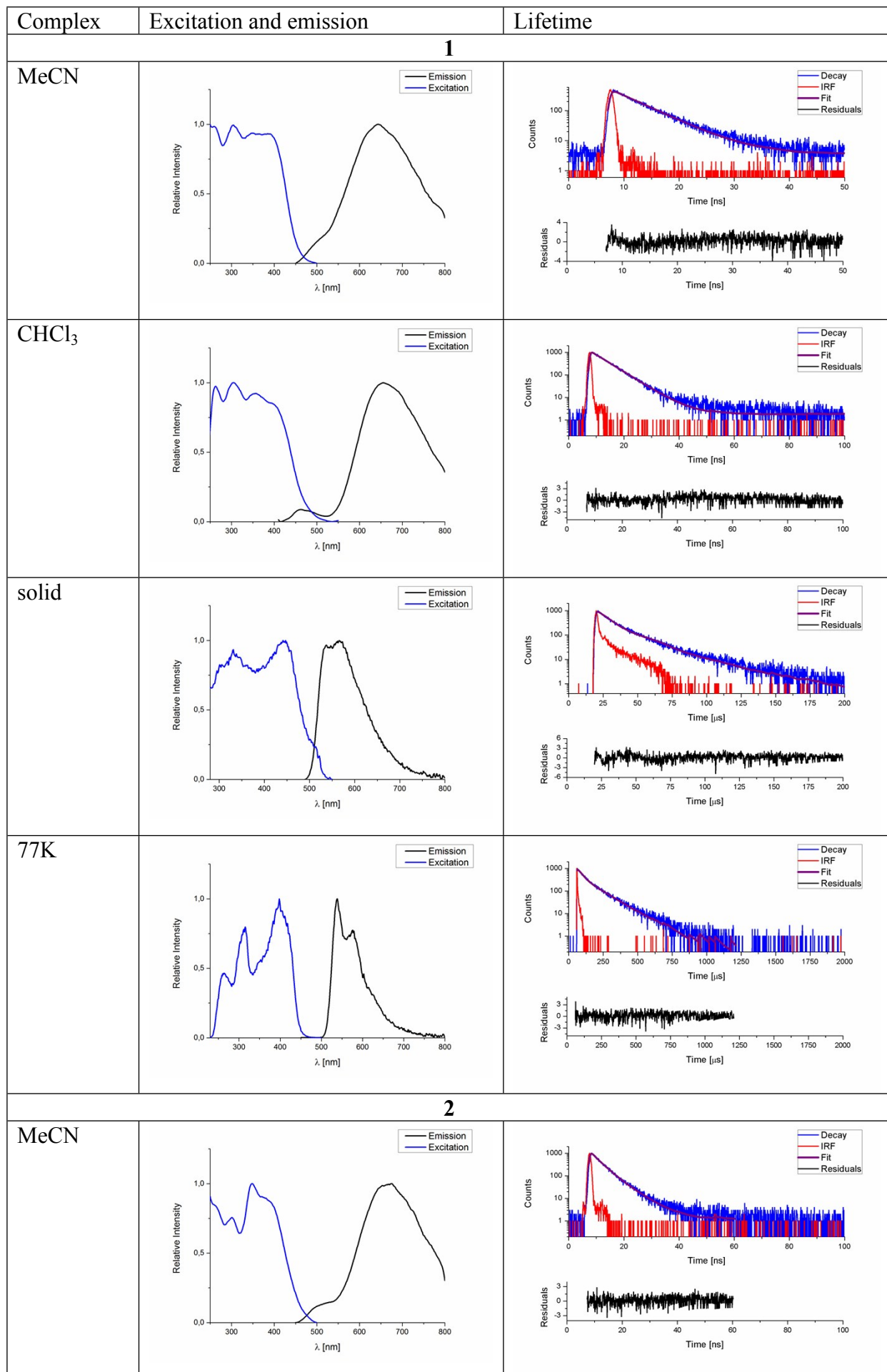
**Figure S3.** Experimental (black) and calculated (red) electronic absorption spectra of **1-6** in MeCN solution.

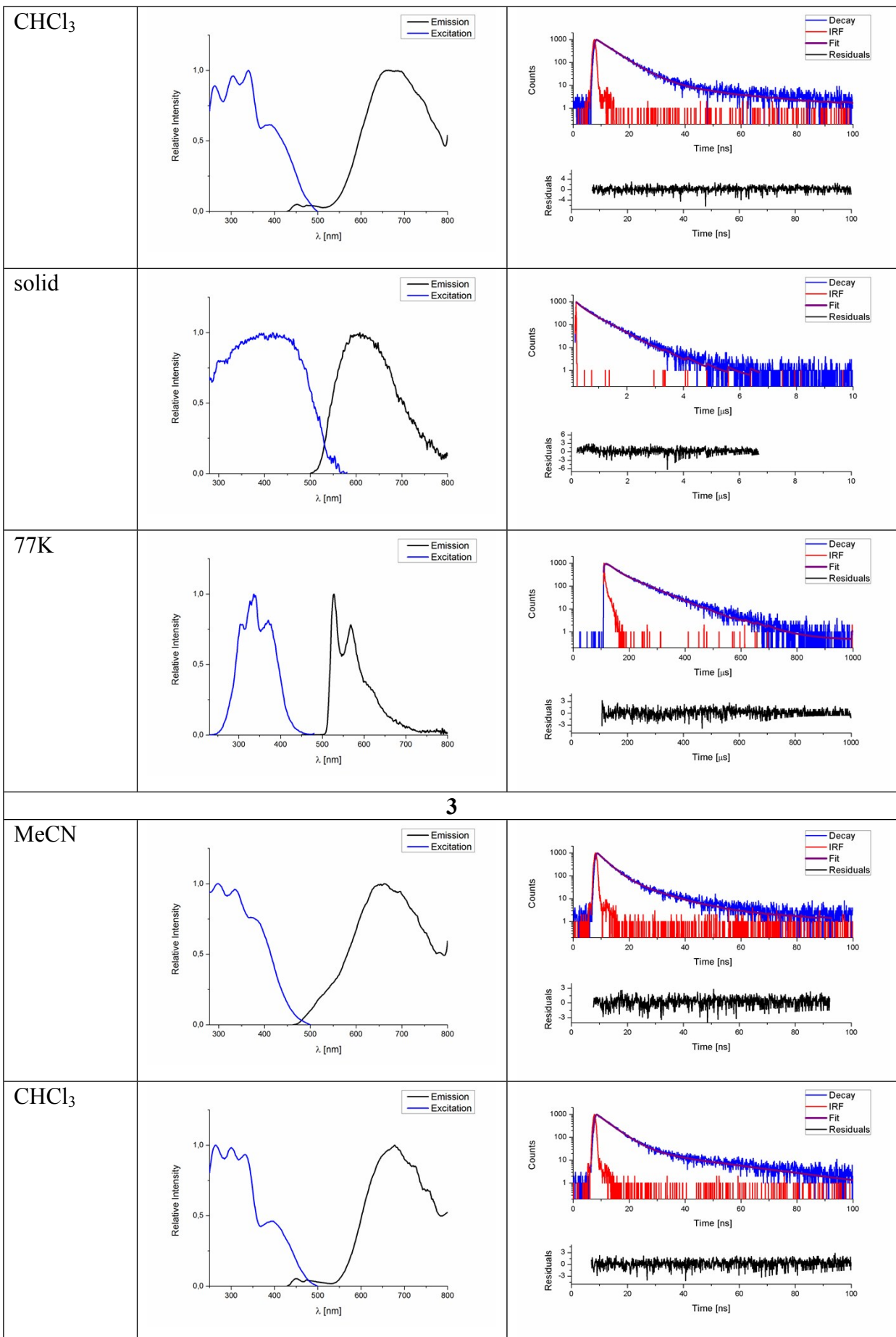
Complex	$\lambda_{\text{cal}}$ [nm]	$\lambda_{\text{exp}}$ [nm]		Hole	Electron
<b>1</b>	421.6	383.8	$S_1$ $W=0.993$		
			$S_2$ $W=0.990$		
<b>2</b>	404.6	383.2	$S_2$ $W=0.991$		
<b>3</b>	410.9	381.0	$S_2$ $W=0.990$		
<b>4</b>	459.6	406.3	$S_1$ $W=0.994$		
			$S_2$ $W=0.996$		

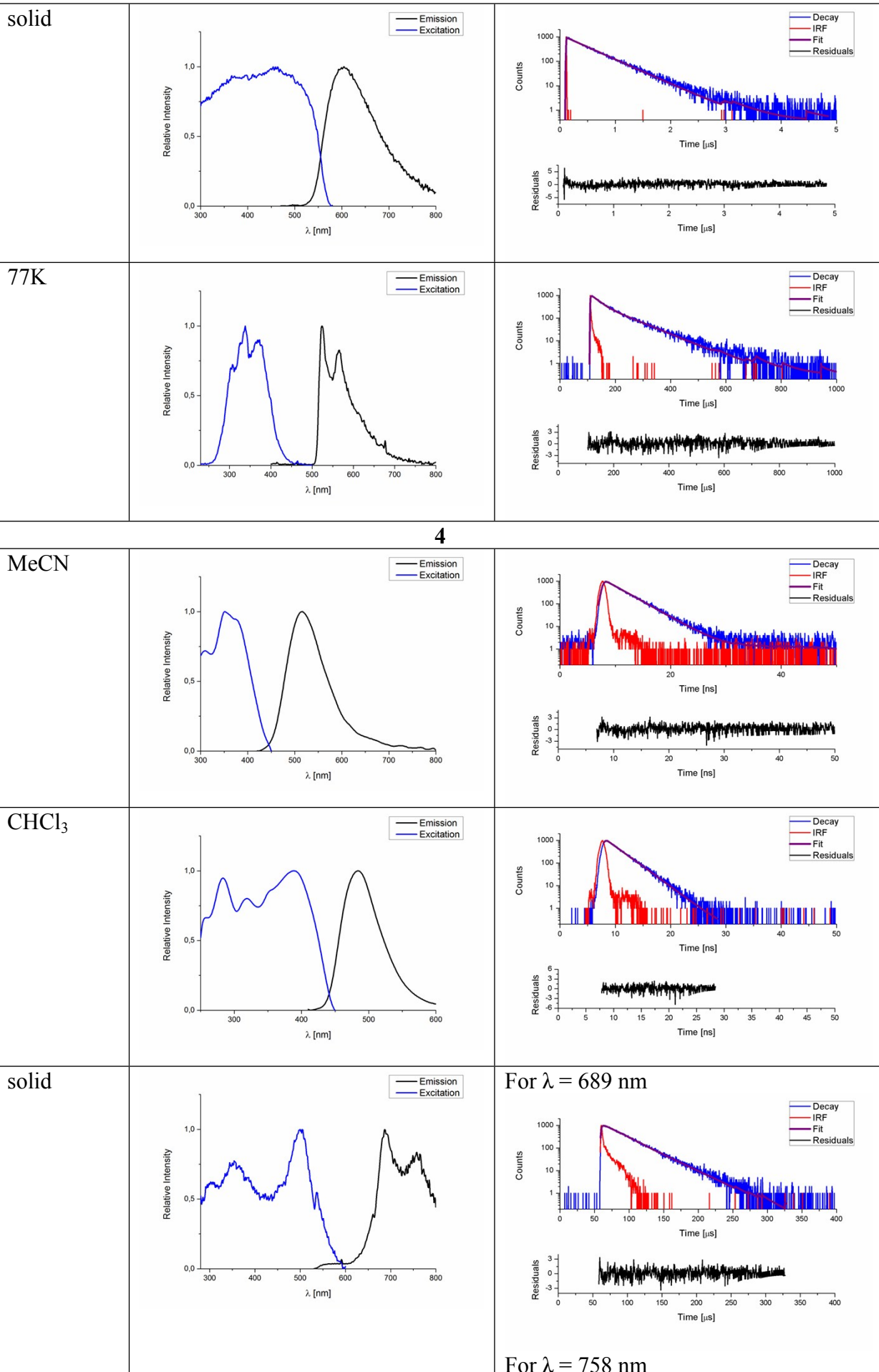
	377.9		$S_4$ $W=0.962$		
<b>5</b>	419.8	383.2	$S_2$ $W=0.991$		
	394.0		$S_3$ $W=0.990$		
<b>6</b>	448.7	386.9	$S_1$ $W=0.996$		
	426.8		$S_2$ $W=0.995$		

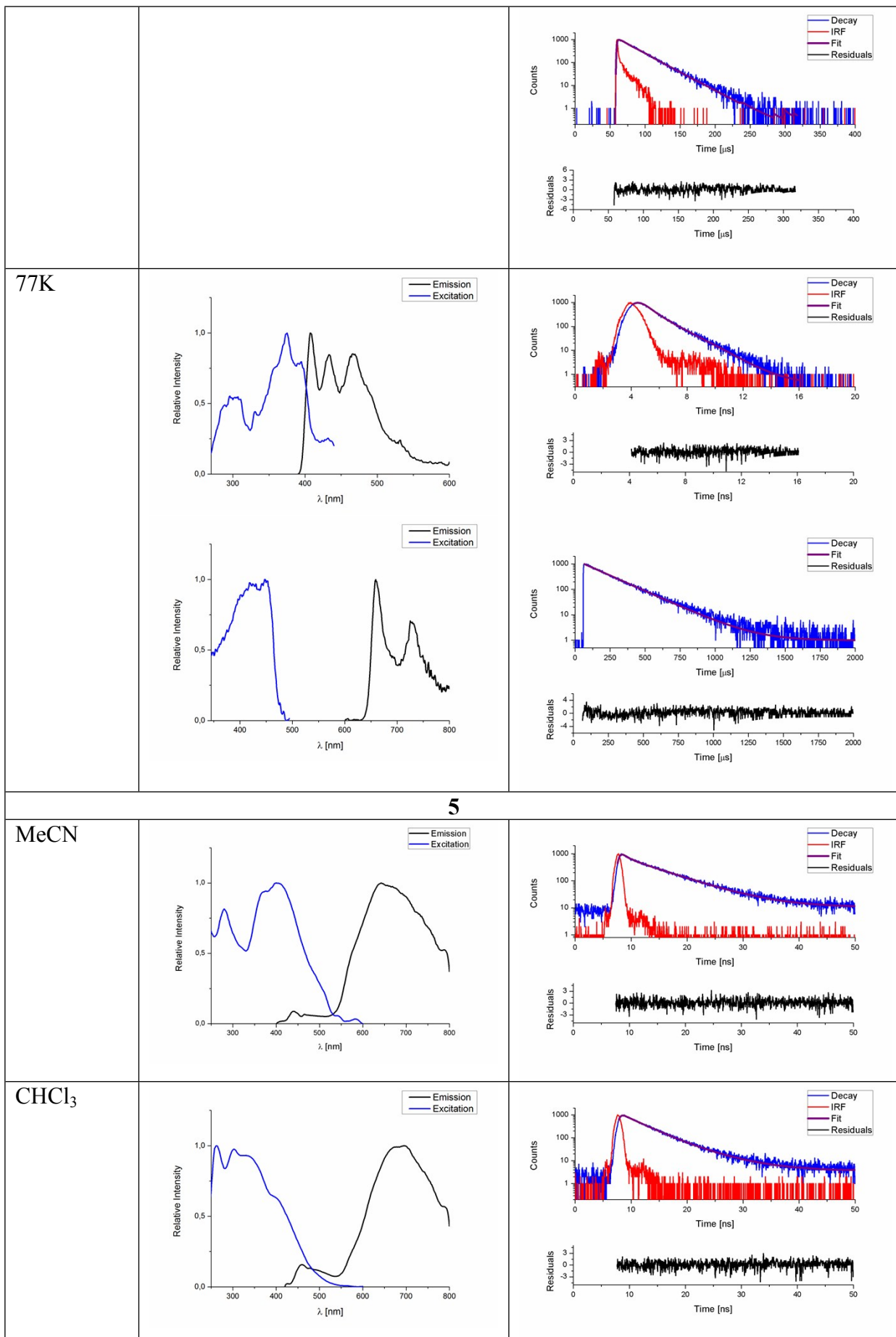
**Figure S4.** Natural transition orbitals (NTOs) of complexes **1-6** illustrating the nature of optically active singlet excited states in the absorption bands.

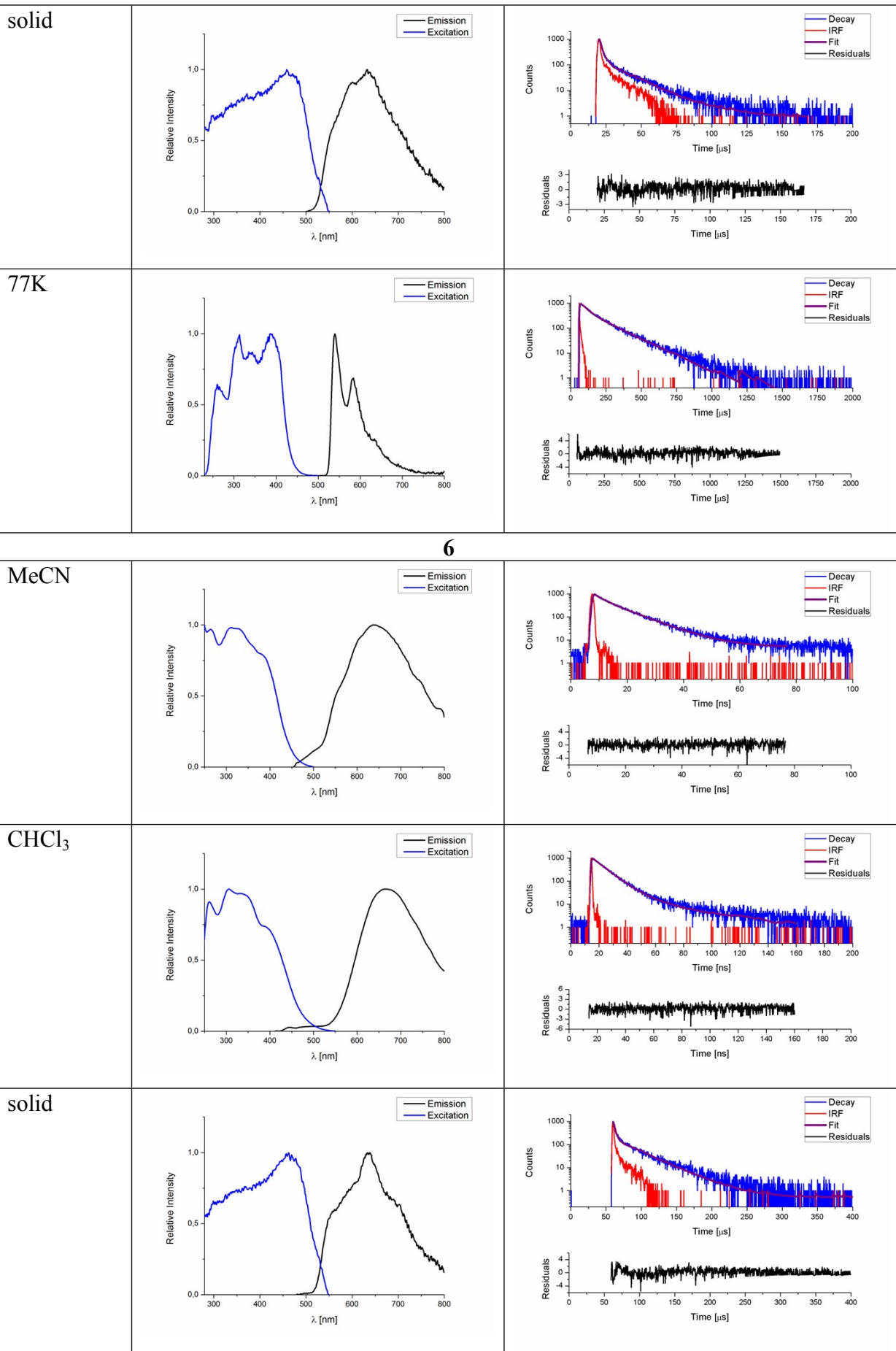












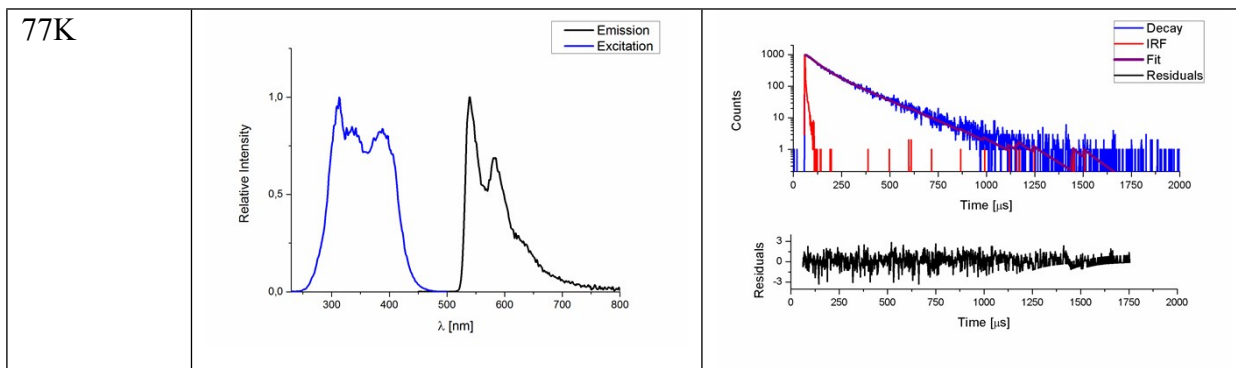


**Figure S5.** Excitation and emission spectra together with PL lifetime curves for **1-6** in  $\text{CH}_2\text{Cl}_2$ ,  $\text{CHCl}_3$ , MeCN and in solid state.

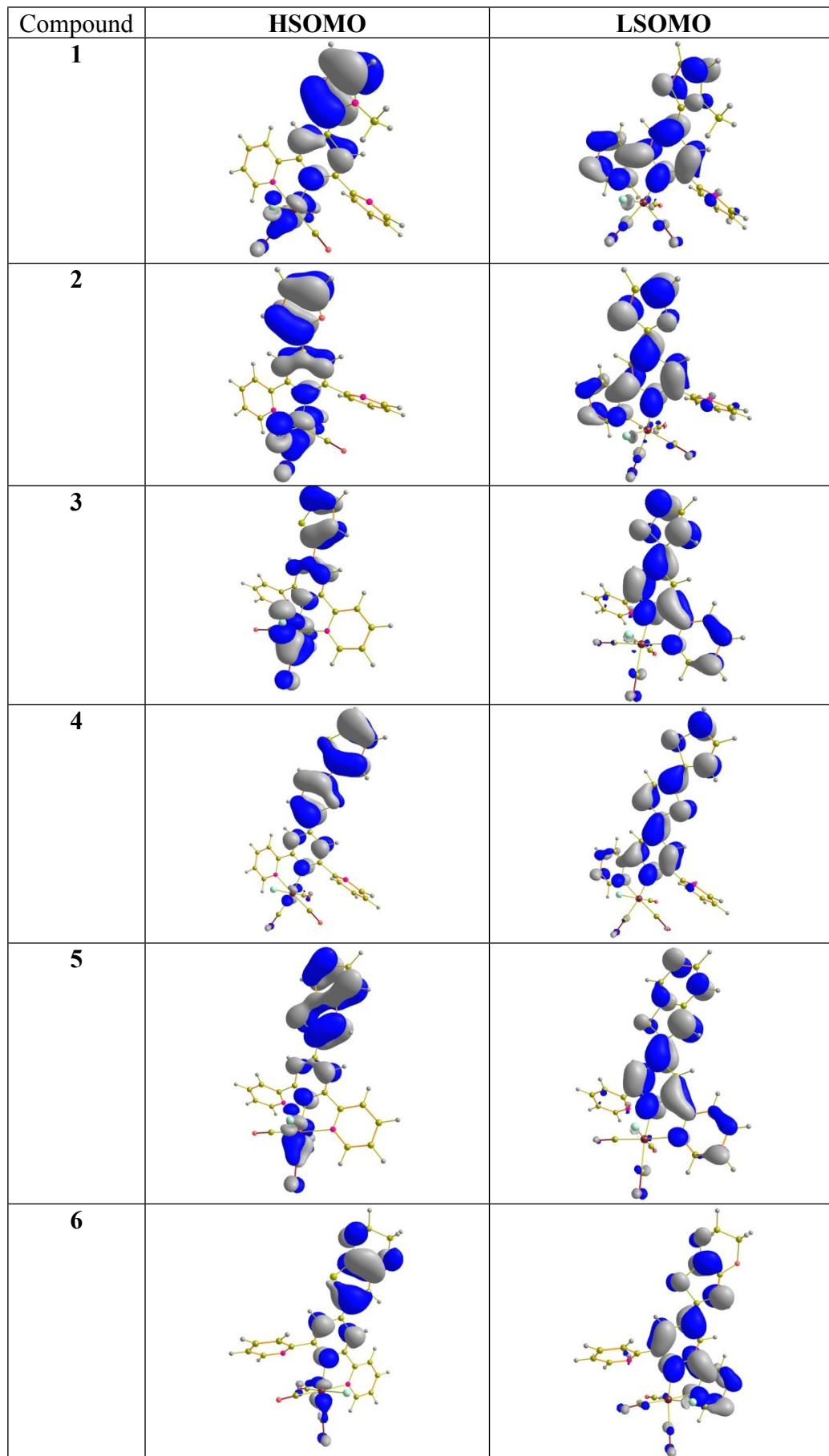


**Figure S6.** Isodensity surface plots of the HSOMO and LSOMO for the complexes **1–6** at their T<sub>1</sub> TDDFT state geometry. Blue and grey colours show regions of positive and negative spin density values, respectively.

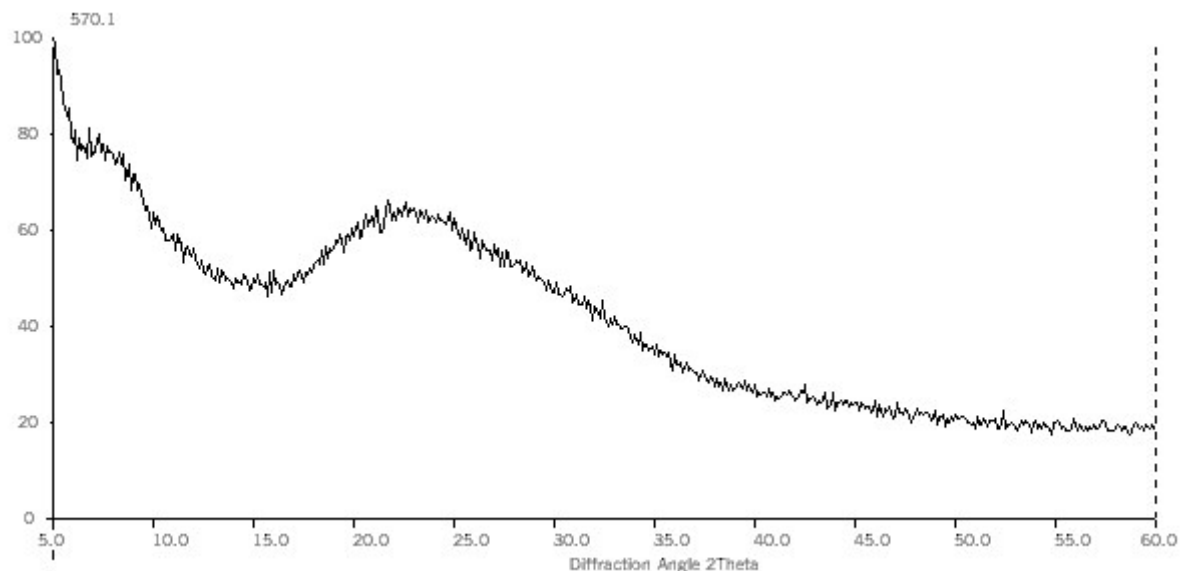


**Figure S7.** X- ray diffraction patterns of blend with 15 % of **1**

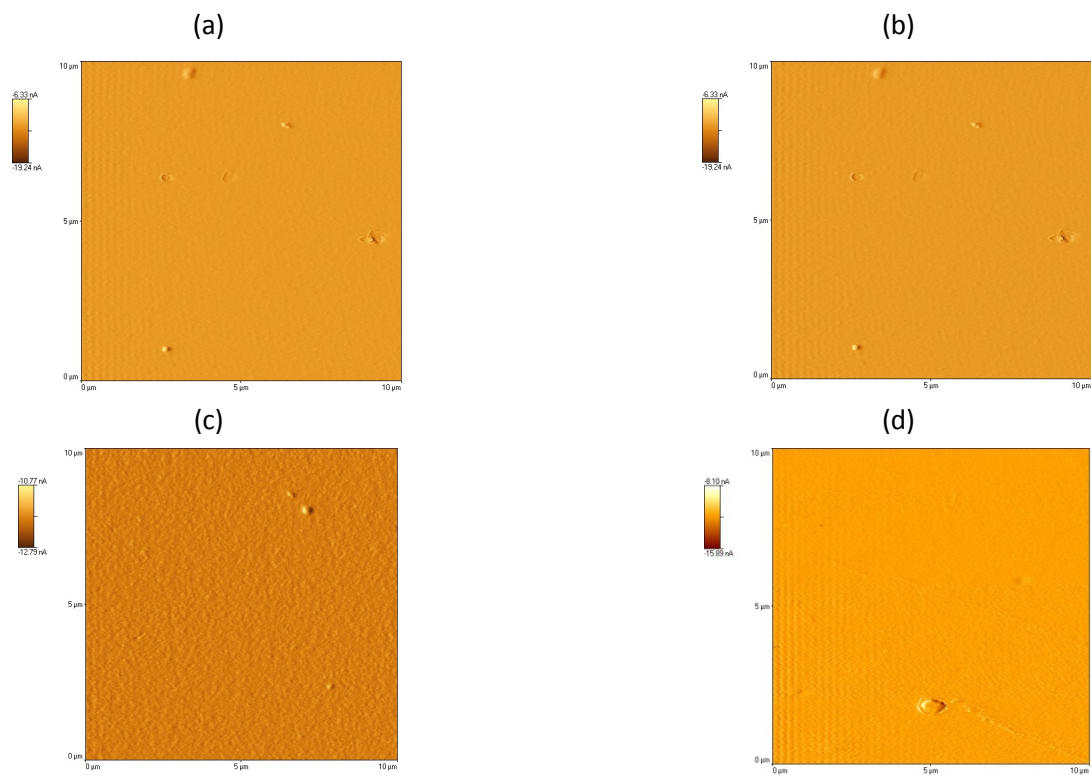


**Figure S8.** AFM images (10  $\mu\text{m}$  x 10  $\mu\text{m}$ ) of 15% doped PVK with (a)  $[\text{ReCl}(\text{CO})_3(4'\text{-R}^1\text{terpy-}\kappa^2\text{N})]$ , (b)  $[\text{ReCl}(\text{CO})_3(4'\text{-R}^4\text{terpy-}\kappa^2\text{N})]$  (c)  $[\text{ReCl}(\text{CO})_3(4'\text{-R}^6\text{terpy-}\kappa^2\text{N})]$  and (d) pure PVK film in devices.